Model Predictive Control with Two-step horizon for Three-level Neutral-Point Clamped inverter

Binh Quang Van Ngo, Pedro Rodriguez-Ayerbe, Sorin Olaru

▶ **To cite this version:**

Binh Quang Van Ngo, Pedro Rodriguez-Ayerbe, Sorin Olaru. Model Predictive Control with Two-step horizon for Three-level Neutral-Point Clamped inverter. 20th International Conference on Process Control, Jun 2015, Štrbské Pleso, Slovakia. pp.215-220, 10.1109/PC.2015.7169965 . hal-01259926

HAL Id: hal-01259926

https://centralesupelec.hal.science/hal-01259926

Submitted on 11 Apr 2020

HAL is a multi-disciplinary open access archive for the deposit and dissemination of scientific research documents, whether they are published or not. The documents may come from teaching and research institutions in France or abroad, or from public or private research centers.

L'archive ouverte pluridisciplinaire **HAL**, est destinée au dépôt et à la diffusion de documents scientifiques de niveau recherche, publiés ou non, émanant des établissements d'enseignement et de recherche français ou étrangers, des laboratoires publics ou privés.

Model Predictive Control with Two-step horizon for Three-level Neutral-Point Clamped inverter

Binh Quang Van Ngo
CentralSupelec, France
Email: Binhvanquang.Ngo@supelec.fr

Pedro Rodriguez-Ayerbe
CentralSupelec, France
Email: Pedro.Rodriguez@supelec.fr

Sorin Olaru
CentralSupelec, France
Email: Sorin.Olaru@supelec.fr

***Abstract*—This paper presents a detailed description of Finite Control Set Model Predictive Control (FCS-MPC) applied to three-level neutral point clamped inverter (3L-NPC). The controller uses a model of the converter, DC link and load to calculate predictions of the future values of the load currents and DC-link capacitor voltages for all possible voltage vectors. The cost function is defined to minimize the error between the reference currents and predicted load currents, balance the DC-link capacitor voltage and reduce the switching frequency. The optimal switching state that minimizes the cost function is selected and applied to the converter. Furthermore, the quality of the current and voltage are improved by using a two prediction steps procedure. Simulation results for the one and two prediction step are presented and compared with linear current controller and space-vector modulation (PI-SVM). The obtained results show the better performances of the proposed control method.**

I. Introduction

In recent years, many industrial applications began demanding high power converters such as new energy systems, high voltage direct current transmission, especially with the development of high power generators using wind power (with the medium voltage and high power level of more than 1 MW). With the development of power electronics, many new multilevel converters have been proposed: diode-clamped (neutral-clamped), flying capacitor and cascaded H-bridge. Among them, three-level neutral point-clamped inverter structure is considered a good solution due to its advantages: reduce the total harmonic distortion (THD), common mode voltage, increase the capacity of the inverter thanks to a decreased voltage applied to each component [1], [3], [4].

Predictive control for power converters and electric drives is a modern control method that has a big potential for application in the power conversion system. Among the advanced control technology, the Model Predictive Control (MPC) is one that has been successfully used in industrial applications because it has several advantages, such as easy inclusion of nonlinearities in the model, constraint and delay compensation. Since the converter has a finite number of switching states, in this case, the control method is known as a finite control set model predictive control (FCS-MPC).

This article proposes an improved FCS-MPC to control the load current for 3L-NPC while maintaining the balance between the DC link capacitor voltage and reducing the switching frequency. These objectives are accomplished through the cost function. First, the discrete-time model of the three-level inverter is established, and then the predicted values of the outputs (current, DC capacitor voltages) for the control variable corresponding to all switching state are estimated. Finally, the optimal switching state with the minimum cost function is selected and applied to the inverter. However, this method has one problem: it needs a high amount of calculations. This makes the calculation time considerable, and increases the delay between the measurements and the actuation. In order to compensate this delay, reduce the amount of calculation and improve the quality of the current, the method proposed in the present paper uses two-step prediction with same voltage vector during two steps, instead of different vectors. A comparison between MPC with one and two-step prediction and PI-SVM for different conditions of references and loads using Matlab/Simulink verify the correctness and feasibility of the proposed method.

This paper is organized as follow: section 2 presents the mathematical model of the three-level inverter. Section 3 explains the proposed control method. In section 4, simulation results are represented and analyzed and finally section 5 draws the conclusion.

II. Model of three-level neutral point clamped inverter

A. Topology

Figure 1 shows a simplified diagram of the three-level neutral point clamped inverter. Each inverter branch is composed of four switches with four anti-parallel diodes. On the DC side of the converter, the DC bus capacitor is divided into two parts, by providing a neutral point Z [1], [3]. The diodes are connected to the neutral point Z, D_{Z11} and D_{Z12} are clamping diodes. The voltage across each of the DC capacitor is normally equal to the half of the total DC voltage U_{dc}. The operating status of 3L-NPC switches can be represented by three switching states [P], [O] and [N]. The switching state [P] or [1] signifies both S_{11} and S_{12} switches in branch A are states "ON" and the inverter terminal voltage U_{AZ} has the value $+U_{dc}/2$, while [N] or [-1] indicates two switches S_{11} and S_{12} are conditions "OFF", leading to $U_{AZ} = -U_{dc}/2$. The switching state [O] or [0] means that the two internal switches S_{11} is "ON" state and S'_{12} is "ON" and U_{AZ} is clamped to zero through the clamping diodes. Taking into account the three phases of the inverter, there are in total 27 possible combinations of switching states corresponding to 19 voltage vectors. Considering the voltage vector definition for the output voltage:

$$u_s = \frac{2}{3}(u_{AZ} + a u_{BZ} + a^2 u_{CZ}) \tag{1}$$

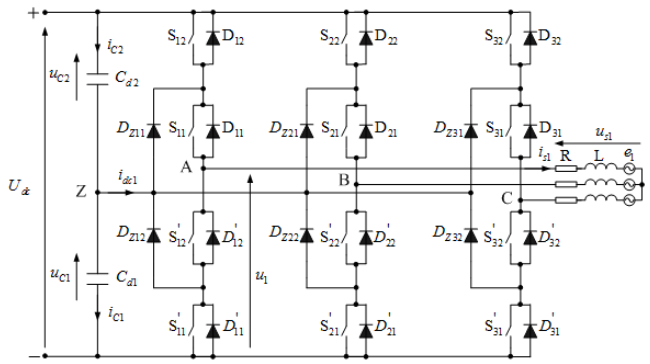

Fig. 1. The configuration of the three-level neutral point clamped inverter

with $a = e^{j2\pi/3} = -\frac{1}{2} + j\frac{\sqrt{3}}{2}$

B. Mathematical model

In order to ensure proper operation of the inverter, the two voltages across the capacitors must be maintained equal to half of the total voltage:

$$u_{C1} = u_{C2} = U_{dc}/2 \tag{2}$$

To clarify the operation of the three-phase inverter, we took the first switching branch (table I) as an example: u_1 is the voltage between the midpoint of the branch and negative voltage. From the analysis, we can express the voltage as follows:

$$u_1 = \sum_{i=1}^{2} S_{1i} u_{Ci} = S_{11} u_{C1} + S_{12} u_{C2} \tag{3}$$

From equation (3), we can express three-phase voltages set in matrix form as below:

$$\begin{bmatrix} u_1 \\ u_2 \\ u_3 \end{bmatrix} = \begin{bmatrix} S_{11} & S_{12} \\ S_{21} & S_{22} \\ S_{31} & S_{32} \end{bmatrix} \begin{bmatrix} u_{C1} \\ u_{C2} \end{bmatrix} \tag{4}$$

TABLE I. THE STATES OF PHASE A OF THE INVERTER

S_a	S_{11}	S_{12}	S'_{11}	S'_{12}	u_1	i_{adc1}
1	1	1	0	0	$u_{C1}+u_{C2}$	0
0	1	0	0	1	u_{C1}	i_{s1}
-1	0	0	1	1	0	0

The voltage on one phase of the load u_{sk} can be written in terms of voltage u_1 to u_3 inverter as follows:

$$\begin{cases} u_{s1} = \frac{1}{3}(2u_1 - u_2 - u_3) \\ u_{s2} = \frac{1}{3}(-u_1 + 2u_2 - u_3) \\ u_{s3} = \frac{1}{3}(-u_1 - u_2 + 2u_3) \end{cases} \tag{5}$$

From equations (4) and (5), the load voltages are expressed in terms of DC link capacitor voltages and switching states as follows:

$$\begin{bmatrix} u_{s1} \\ u_{s2} \\ u_{s3} \end{bmatrix} = \begin{bmatrix} S_{C11} & S_{C12} \\ S_{C21} & S_{C22} \\ S_{C31} & S_{C32} \end{bmatrix} \begin{bmatrix} u_{C1} \\ u_{C2} \end{bmatrix} \tag{6}$$

Where

$$\begin{cases} S_{C11} = \frac{1}{3}(2S_{11} - S_{21} - S_{31}) \\ S_{C12} = \frac{1}{3}(2S_{12} - S_{22} - S_{32}) \\ S_{C21} = \frac{1}{3}(-S_{11} + 2S_{21} - S_{31}) \\ S_{C22} = \frac{1}{3}(-S_{12} + 2S_{22} - S_{32}) \\ S_{C31} = \frac{1}{3}(-S_{11} - S_{21} + 2S_{31}) \\ S_{C32} = \frac{1}{3}(-S_{12} - S_{22} + 2S_{32}) \end{cases} \tag{7}$$

The equation of current with load RL and electromotive force (EMF) can be written as:

$$\begin{aligned} Ri_{s1} + L\frac{di_{s1}}{dt} + e_1 &= u_{s1} \\ \frac{di_{s1}}{dt} &= -\frac{R}{L} i_{s1} + \frac{1}{L}(u_{s1} - e_1) \end{aligned} \tag{8}$$

Or we can express three-phase currents set in matrix form as below:

$$\frac{d}{dt}\begin{bmatrix} i_{s1} \\ i_{s2} \\ i_{s3} \end{bmatrix} = \begin{bmatrix} -R/L & 0 & 0 & S_{C11}/L & S_{C12}/L \\ 0 & -R/L & 0 & S_{C21}/L & S_{C22}/L \\ 0 & 0 & -R/L & S_{C31}/L & S_{C32}/L \end{bmatrix} \begin{bmatrix} i_{s1} \\ i_{s2} \\ i_{s3} \\ u_{C1} \\ u_{C2} \end{bmatrix} + \begin{bmatrix} -1/L & 0 & 0 \\ 0 & -1/L & 0 \\ 0 & 0 & -1/L \end{bmatrix} \begin{bmatrix} e_1 \\ e_2 \\ e_3 \end{bmatrix} \tag{9}$$

On other hand, the neutral current i_{dc1} can be calculated from three-phase load currents and the switching states as follows (Fig. 1):

$$\begin{aligned} i_{dc1} &= (S_{11} - S_{12})i_{s1} + (S_{21} - S_{22})i_{s2} + (S_{31} - S_{32})i_{s3} \\ &= i_{c2} - i_{c1} = H_{s1}i_{s1} + H_{s2}i_{s2} + H_{s3}i_{s3} \end{aligned} \tag{10}$$

Where H_{s1} = 1 when S_{11} = 1, S_{12} = 0, otherwise H_{s1} = 0

Assuming that the DC bus voltage U_{dc} is constant and C_{d1} = C_{d2} = C:

$$i_{c1} = C\frac{du_{C1}}{dt} = C\frac{d(U_{dc} - u_{C2})}{dt} = -C\frac{du_{C2}}{dt} = -i_{c2} \tag{11}$$

By substituting equation (10) into equation (11), the DC-link capacitor voltages are expressed as follows:

$$\begin{aligned} \frac{du_{C1}}{dt} &= -\frac{1}{2C}(H_{s1}i_{s1} + H_{s2}i_{s2} + H_{s3}i_{s3}) \\ \frac{du_{C2}}{dt} &= \frac{1}{2C}(H_{s1}i_{s1} + H_{s2}i_{s2} + H_{s3}i_{s3}) \end{aligned} \tag{12}$$

Based on equation (9) and (12), the three-phase currents and the DC-link capacitor voltages can be expressed in matrix form

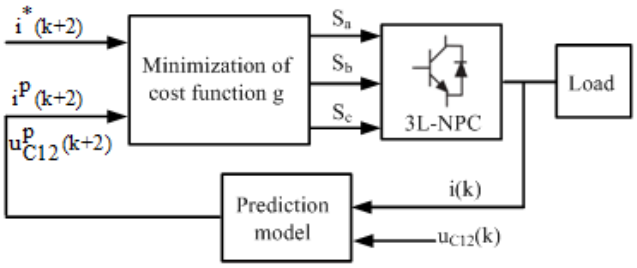

Fig. 2. Predictive current control block diagram for 3L-NPC inverter

as below:

$$\frac{d}{dt}\begin{bmatrix} i_{s1} \\ i_{s2} \\ i_{s3} \\ u_{C1} \\ u_{C2} \end{bmatrix} = \begin{bmatrix} -R/L & 0 & 0 & S_{C11}/L & S_{C12}/L \\ 0 & -R/L & 0 & S_{C21}/L & S_{C22}/L \\ 0 & 0 & -R/L & S_{C31}/L & S_{C32}/L \\ -K_1 & -K_2 & -K_3 & 0 & 0 \\ K_1 & K_2 & K_3 & 0 & 0 \end{bmatrix} \begin{bmatrix} i_{s1} \\ i_{s2} \\ i_{s3} \\ u_{C1} \\ u_{C2} \end{bmatrix} + \begin{bmatrix} -1/L & 0 & 0 \\ 0 & -1/L & 0 \\ 0 & 0 & -1/L \\ 0 & 0 & 0 \\ 0 & 0 & 0 \end{bmatrix} \begin{bmatrix} e_1 \\ e_2 \\ e_3 \end{bmatrix} \quad (13)$$

Where

$$\begin{cases} K_1 = \dfrac{1}{2C}(S_{11} - S_{12}) \\ K_2 = \dfrac{1}{2C}(S_{21} - S_{22}) \\ K_3 = \dfrac{1}{2C}(S_{31} - S_{32}) \end{cases} \quad (14)$$

III. The application of MPC to 3L-NPC inverter

The FCS-MPC controller predicts the behavior of the inverter for finite possible voltage vector on each sampling interval. A cost function is used to evaluate the voltage vector for the next sampling interval based on the prediction model. The optimal switching time is selected and applied to the inverter during the next sampling period which minimizes the cost function. The schematic MPC is shown in Fig. 2.

The aim of the current control scheme is to minimize the error between the predicted current and the reference values, to maintain voltage balance of the capacitor and to reduce the switching frequency. The cost function for 3L-NPC has the following compositions [2], [4], [6]:

$$g = (i_\alpha^* - i_\alpha^p)^2 + (i_\beta^* - i_\beta^p)^2 + \lambda_{dc}|\, u_{C1}^p - u_{C2}^p| \; + \lambda_n n_c \quad (15)$$

Where i_α^p and i_β^p are the real and imaginary components of the predicted current; i_α^* and i_β^* are the real and imaginary components of the reference current. n_c is the number of switching change when the switching state S(k) is applied compared with previous state S(k-1). It can be expressed as follows:

$$n_c = |\, S_a(k) - S_a(k-1)| \; + |\, S_b(k) - S_b(k-1)| + |\, S_c(k) - S_c(k-1)| \quad (16)$$

where S_x represents the state of a switch and has three states: [-1, 0, 1].

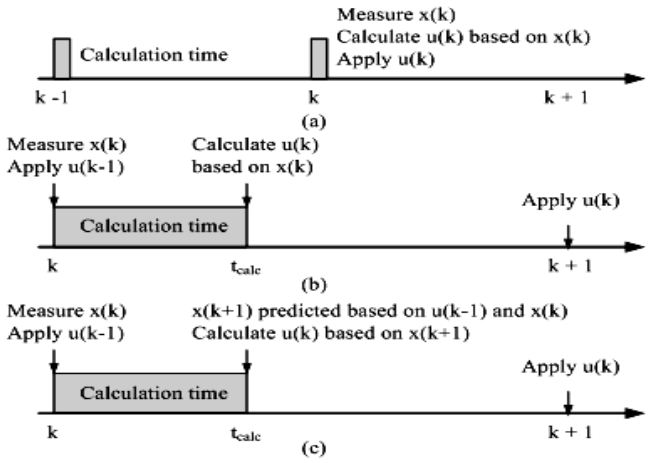

Fig. 3. Operation of the predictive control [5] (a) Ideal case. (b) Real case without time delay compensation. (c) Real case with time delay compensation

And λ_{dc}, λ_n are the weighting factor of the capacitor voltage balancing and the reduction of commutation.

In the ideal case, the time requires for the calculation can be ignored. The operation of predictive control is shown in Fig. 3(a). The states of the systems x(k) are measured at the time k, the optimal switching state is calculated immediately. The switching state that has the smallest error value at the time k+1 is chosen and applied at the time k. On the contrary, in real time the computation time can not be ignored; the control variable u(k) is available late after a sampling period (Fig. 3(b)). At the beginning of sampling k, the state variables x(k) are measured and the calculation of the new value for the control variable is started. The calculation is completed at the time $k + t_{cal}$. So, the updating of the control variable will be applied at k+1.

A simple solution to compensate this delay is to consider the time of calculation and apply the switching state after the next sampling (Fig. 3(c)). The state variables x(k+1) are estimated based on the control variable u(k-1) and the measured system states x(k). u(k-1) is known since it was calculated in the previous sample. Therefore, the model of the inverter is used to estimate x(k+1) at the beginning of the optimization process. Then, the control variable u(k) which is applied at the time k+1, is calculated in the optimization process. As a result, the optimization is executed at the time k+2. In this way, the time delay that exists in the digital control system can be compensated [4], [5].

The possible number (N_t) of trajectory of voltage vector with different switching state (m) and the prediction horizon (n) can be expressed as follows:

$$N_t = m^n \quad (17)$$

There are 27 voltage vectors which are calculated with the prediction horizon (n=1). When two steps are considered for prediction, one voltage vector is applied in the first sampling period, another vector is imposed during the next sampling period. In this case, there are 729 possible trajectories of the vector voltage. Consequently, it leads to large number of performance evaluations and make them difficult to implement the algorithm in practice. In order to reduce the number of

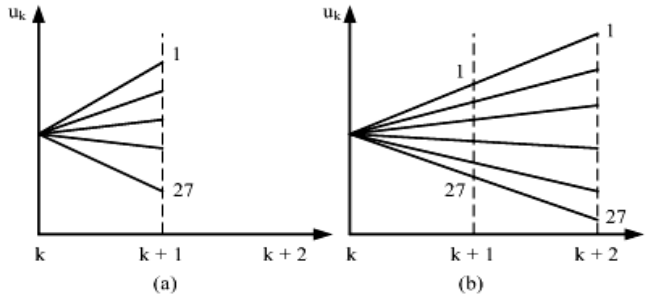

Fig. 4. Control variable prediction for the 3L-NPC inverter (a) One-step prediction. (b) Modified two-step prediction

calculations, we can consider applying the same voltage vector in two-step horizon, instead of different vectors (Fig. 4). This represents practically a move-blocking strategy and allows evaluating the impact of the control on a longer time windows.

As shown in Fig. 2, the cost function requires predicted load current $i^p(k+2)$ and capacitor voltages $u^p_{c1}(k+2)$, $u^p_{c2}(k+2)$ in discrete-time form. Therefore, the first-order forward Euler approximation was used to obtain a discrete-time system representation. The differential state variable is approximated as follows:

$$\frac{dx}{dt} = \frac{x(k+1) - x(k)}{T_s} \tag{18}$$

Approaching equation (8) with equation (18), the load currents are represented in discrete-time as follows:

$$\begin{cases} i^p(k+1) = \left(1 - \frac{RT_s}{L}\right) i(k) + \frac{T_s}{L}\left(u_s(k) - \hat{e}(k)\right) \\ i^p(k+2) = \left(1 - \frac{RT_s}{L}\right) i(k+1) + \frac{T_s}{L}\left(u_s(k) - \hat{e}(k+1)\right) \end{cases} \tag{19}$$

Where $\hat{e}(k)$ represents the estimated back-EMF. We can calculate back-EMF based on equation (8) as follows:

$$\hat{e}(k-1) = u_s(k-1) - \frac{L}{T_s} i(k) - \left(R - \frac{L}{T_s}\right) i(k-1) \tag{20}$$

where $\hat{e}(k-1)$ is the estimated value of $\hat{e}(k)$ (because the frequency of EMF is smaller than sampling frequency). Similarly, we have the discrete-time form for the capacitor voltages as follows:

$$\begin{cases} u_{C1}(k+1) = u_{C1}(k) + \dfrac{1}{C} i_{c1}(k) T_s \\ u_{C2}(k+1) = u_{C2}(k) + \dfrac{1}{C} i_{c2}(k) T_s \end{cases} \tag{21}$$

where i_{c1}, i_{c2} depend the switching states and the output currents, and can be calculated by using the following expression:

$$\begin{cases} i_{c1}(k) = -\dfrac{1}{2}\left(H_{s1} i_{s1}(k) + H_{s2} i_{s2}(k) + H_{s3} i_{s3}(k)\right) \\ i_{c2}(k) = \dfrac{1}{2}\left(H_{s1} i_{s1}(k) + H_{s2} i_{s2}(k) + H_{s3} i_{s3}(k)\right) \end{cases} \tag{22}$$

The DC-link capacitor voltages for two-step prediction are obtained by shifting variable into one future sample. Then, it can be expressed as follows:

$$\begin{cases} u_{C1}(k+2) = u_{C1}(k+1) + \frac{1}{C} i_{c1}(k+1) T_s \\ u_{C2}(k+2) = u_{C2}(k+1) + \frac{1}{C} i_{c2}(k+1) T_s \end{cases} \tag{23}$$

Where

$$\begin{cases} i_{c1}(k+1) = -\dfrac{1}{2} \sum_{i=1}^{3} (H_{si} i_{si}(k+1)) \\ i_{c2}(k+1) = -i_{c1}(k+1) \end{cases} \tag{24}$$

Hence, the cost function of MPC for the 3L-NPC inverter with one step prediction can be expressed as:

$$g = \left(i^*_\alpha(k+1) - i^p_\alpha(k+1)\right)^2 + \left(i^*_\beta(k+1) - i^p_\beta(k+1)\right)^2 + \lambda_{dc} \left| u^p_{C1}(k+1) - u^p_{C2}(k+1) \right| + \lambda_n n_c \tag{25}$$

The expression of the cost function with two-step prediction can be written as follows:

$$g = \left(i^*_\alpha(k+1) - i^p_\alpha(k+1)\right)^2 + \left(i^*_\beta(k+1) - i^p_\beta(k+1)\right)^2 + \left(i^*_\alpha(k+2) - i^p_\alpha(k+2)\right)^2 + \left(i^*_\beta(k+2) - i^p_\beta(k+2)\right)^2 + \lambda_{dc} \left| u^p_{C1}(k+2) - u^p_{C2}(k+2) \right| + \lambda_n n_c \tag{26}$$

The future currents $i^*(k+1)$, $i^*(k+2)$ are estimated by extrapolation using Lagrange method based on the present and passed value. This process can be expressed as follows:

$$\begin{array}{rcl} i^*(k+1) & = & 3i^*(k) - 3i^*(k-1) + i^*(k-2) \\ i^*(k+2) & = & 6i^*(k) - 8i^*(k-1) + 3i^*(k-2) \end{array} \tag{27}$$

IV. Simulation results

To evaluate the quality performance, we can use the mean square error (MSE). It can be express as follows:

$$MSE = \frac{1}{n} \sum_{i=1}^{n} \left(y^*_i - y^p_i\right)^2 \tag{28}$$

where y^*_i is the reference vector and y^p_i is the vector of prediction.

On other hand, in order to estimate the average switching frequency per semiconductor ($\overline{f_{sw}}$) of FCS-MPC, the following expression can be used [2], [4]:

$$\overline{f_{sw}} = \sum_{i=1}^{4} \frac{f_{s_{ai}} + f_{s_{bi}} + f_{s_{ci}}}{12} \tag{29}$$

where f_{ski} is the average switching frequency during a time interval of power switching number i of phase k, with i $\in \{1,2,3,4\}$ and k $\in \{a,b,c\}$.

The proposed predictive control is analyzed and compared with linear current controller and space vector modulation (PI-SVM). The parameters of inverter is summarized in table II.

To generate the same average switching frequency per semiconductor, the sampling frequency of the FCS-MPC is considered $f_s = 10kHz$ and the sampling frequency of the SVM is 5 kHz. For the SVM at 5 kHz, $\overline{f_{sw}} = 2.5kHz$ and

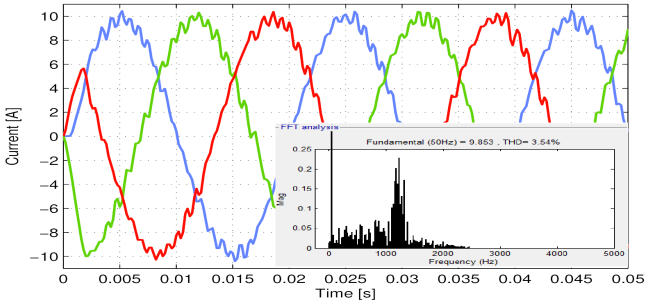

Fig. 5. The transient response and THD of three-phase current for PI-SVM

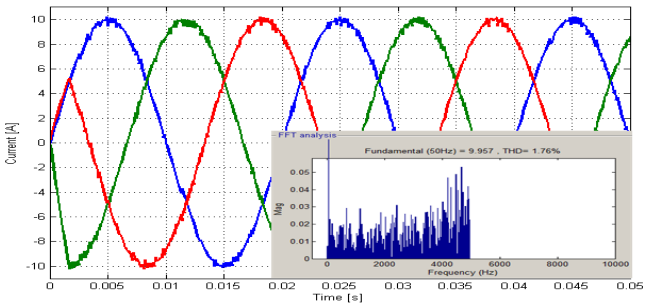

Fig. 6. The transient response and THD of three-phase current for FCS-MPC

the expected value of $\overline{f_{sw}}$ for FCS-MPC is about 2.5 kHz. The transient responses of the PI-SVM and MPC from zero load current until the steady state and the total harmonic distortion (THD) are illustrated in Fig. 5 and Fig. 6. In order to observe the dynamics ability to track the current reference and the interaction between two components of the load current, the amplitude of the current reference steps from 10 A to 5 A (Fig. 7(a)), then steps from 5 A to 10 A (Fig. 7(b)) at t = 0.065 [s]. The mean square error of PI-SVM is 0.336 and 0.097 with MPC. From the results presented, it is clear that the predictive method obtains an accurate current tracking ability with a low THD and low current ripple. In addition, it has a fast dynamic response (the corresponding computation time of the algorithm were 0.07msec) with inherent decoupling between two components: real and imaginary (Fig. 8).

One of the important issues of 3L-NPC structure is the balancing voltage of the DC-link capacitor. It is obvious that the voltage of DC-link capacitor remains balanced in spite of the transition of the current reference (Fig. 9).

To compare a MPC with one-step with two-step proposed, we can analyze the characteristic with the load RL with weighting value $\lambda_{dc} = 0.45$ and $\lambda_n = 0.001$ in equation

TABLE II. THE PARAMETERS USED FOR SIMULATION

Parameter	Value	Description
U_{dc}	540 [V]	DC-link voltage
C	1 [mF]	DC-link capacitor
R	10 [Ω]	Load resistance
L	50 [mH]	Load inductance
f_s	10 [kHz]	Sampling frequency for FCS-MPC
f_{svm}	5 [kHz]	Sampling frequency for PI-SVM
f	50 [Hz]	Current reference frequency
E	100 [V]	Back-EMF peak amplitude
I_{ref}	10 [A]	Peak amplitude of reference current

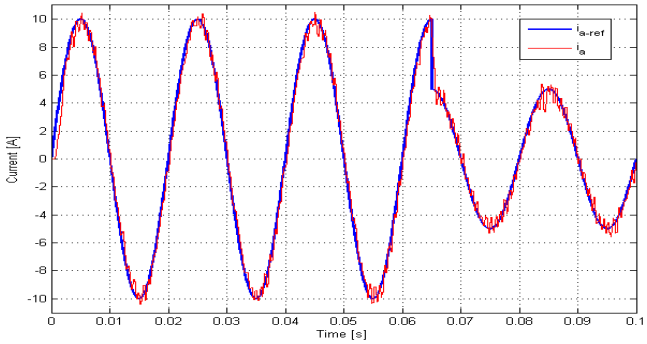

(a) PI-SVM

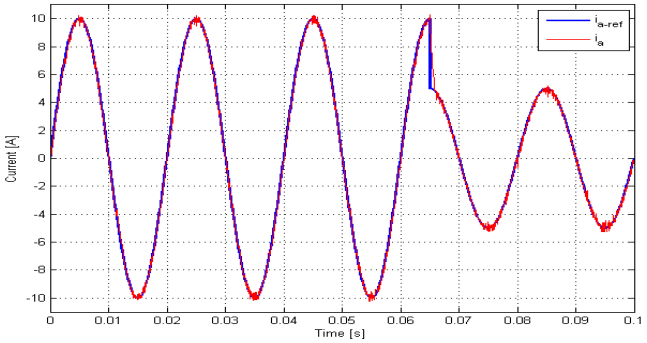

(b) FCS-MPC

Fig. 7. The load curent transient response for a reference step of 10A-5A

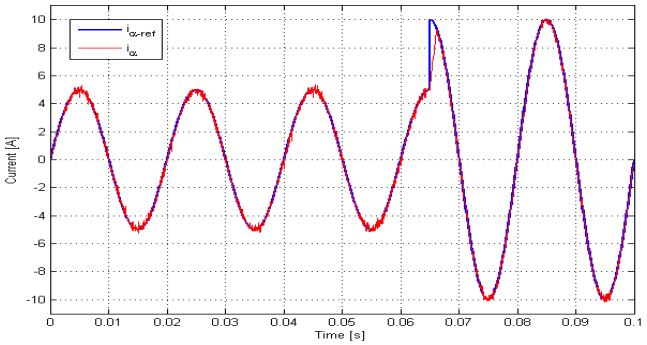

(a) In the coordinate α

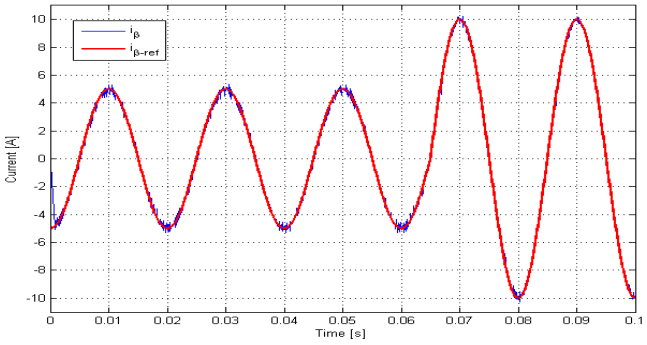

(b) In the coordinate β

Fig. 8. The load curent response for a reference step of 5A-10A

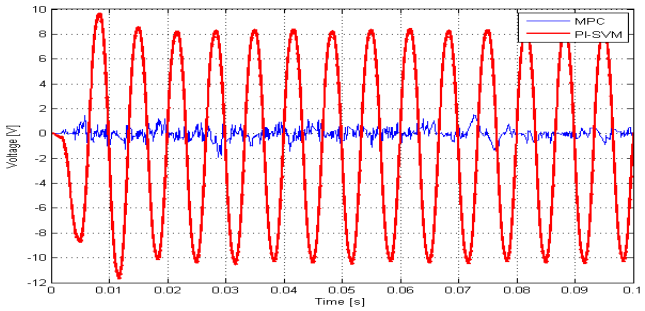

Fig. 9. The difference between the DC-link capacitor voltage

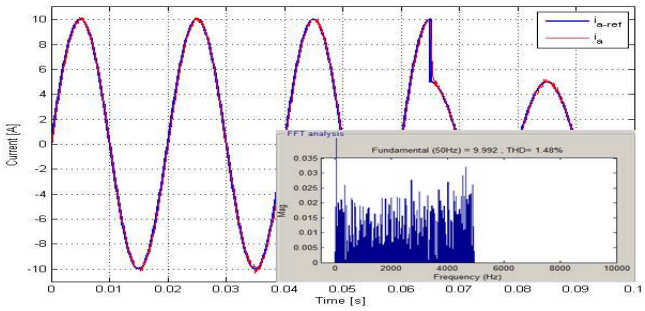

Fig. 10. The load current response with one-step prediction

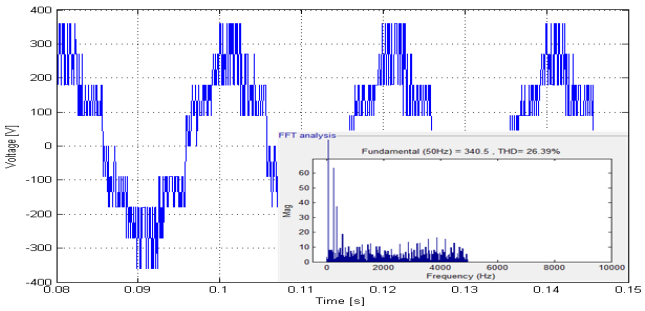

Fig. 12. The load voltage in one phase of proposed method

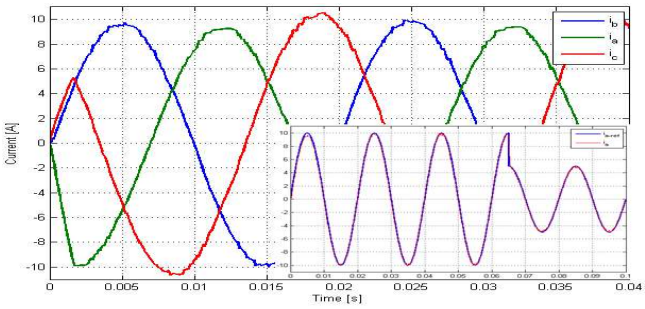

Fig. 13. The load current response of proposed method with unbalanced load

(25). The load current with one-step prediction, which is illustrated in Fig. 10, creates 1.48% THD. The average switching frequency $\overline{f_{sw}}$ is 1280 Hz. The load current with two-step prediction, which is shown in Fig. 11, creates 1.21% THD, and respectively 883 Hz. Hence, this method provides a new approach to control high power converter that require an operation with lower switching frequency. Furthermore, the THD of the voltage of proposed method (26.39%) is smaller than MPC with one-step prediction (28.01%). The operating condition discussed is repeated with unbalanced load ($R_a = 12\Omega, R_b = 10\Omega, R_c = 8\Omega$). Fig. 13 shows that the load currents effectively follow their references with the unbalancing load.

V. Conclusions

This study proposes an FCS-MPC strategy with one and two steps prediction for 3L-NPC inverter. First, the mathematical model of 3L-NPC inverter is established, and then the cost function, which contains the current error, the capacitor voltage balancing and the reduction of the switching frequency, is established. In this paper, there is a comparison between PI-SVM and FCS-MPC for 3L-NPC inverter. The simulation results show that the algorithm can successfully maintain their balanced capacitor voltages and reduce the switching frequency. In addition, by using proposed method we can reduce the switching frequency and high number of calculations while maintaining an acceptable quality of current and voltage. The control strategy also allows compensating the delay time and the change of load parameters, while the load current continues effective tracking to their references. The linear PI controllers and the modulation block are further eliminated. Therefore, the proposed method is an interesting alternative to control the 3L-NPC converter.

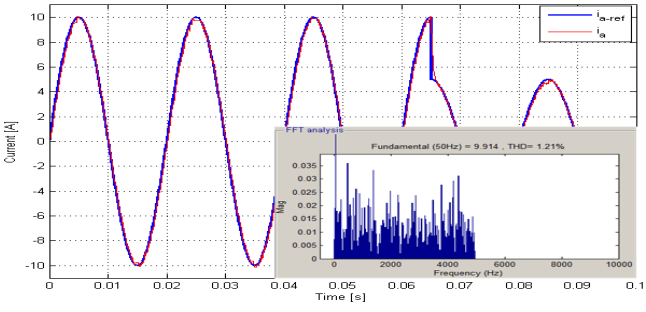

Fig. 11. The load current response with proposed method

References

[1] Marco Liserre Frede Blaabjerg and Ke Ma. Power electronics converters for wind turbine systems. *IEEE Transaction On Industrial Electronics*, 48(2):708–719, 2012.

[2] J. Rodriguez H. Young, M. Perez and H. Abu-Rub. Assessing finite-control-set model predictive control: A comparison with a linear current controller in two-level voltage source inverters. *IEEE Industrial Electronics Magazine*, 8(1):44–52, 2014.

[3] Jamel Belhadj Mohamed Abbes and Ben Abdelghani Bennan. Design and control of a direct drive wind turbine equipped with multilevel converters. *Renewable Energy*, 35:936–945, 2010.

[4] Jose Rodriguez and Patricio Cortes. *Predictive Control of Power Converters and Electrical Drives*. John Wiley, 2012.

[5] Peter Johannes Stolze. *Advanced Finite-Set Model Predictive Control for Power Electronics and Electrical Drives*. Technischen Universitet Munchen, Munich, Germany, 2014.

[6] Mehdi Narimani Bin Wu Venkata Yaramasu, Marco Rivera and Jose Rodriguez. Finite state model-based predictive current control with two-step horizon for four-leg npc converters. *Journal of Power Electronics*, 14(6):1178–1188, 2014.